

Understanding and Accelerating Neural Architecture Search with Training-Free and Theory-Grounded Metrics

Wuyang Chen*, Xinyu Gong*, Yunchao Wei, Humphrey Shi, Zhicheng Yan, Yi Yang, and Zhangyang Wang

Abstract—This work targets designing a principled and unified training-free framework for Neural Architecture Search (NAS), with high performance, low cost, and in-depth interpretation. NAS has been explosively studied to automate the discovery of top-performer neural networks, but suffers from heavy resource consumption and often incurs search bias due to truncated training or approximations. Recent NAS works [1], [2], [3] start to explore indicators that can predict a network’s performance without training. However, they either leveraged limited properties of deep networks, or the benefits of their training-free indicators are not applied to more extensive search methods. By rigorous correlation analysis, we present a unified framework to understand and accelerate NAS, by disentangling “TEG” characteristics of searched networks – *Trainability*, *Expressivity*, *Generalization* – all assessed in a training-free manner. The TEG indicators could be scaled up and integrated with various NAS search methods, including both supernet and single-path approaches. Extensive studies validate the effective and efficient guidance from our TEG-NAS framework, leading to both improved search accuracy and over $2.3\times$ reduction in search time cost. Moreover, we visualize search trajectories on three landscapes of “TEG” characteristics, observing that while a good local minimum is easier to find on NAS-Bench-201 given its simple topology, balancing “TEG” characteristics is much harder on the DARTS search space due to its complex landscape geometry. Our code is available at <https://github.com/VITA-Group/TEGNAS>.

Index Terms—Neural Architecture Search, Neural Tangent Kernel, Linear Region, Generalization

1 INTRODUCTION

THE development of deep convolutional neural networks significantly contributes to the success of computer vision tasks [4], [5], [6], [7]. However, manually designing new network architectures not only costs tremendous time and resources, but also requires a rich network training experience that can hardly scale up. Neural architecture search (NAS) is recently explored to remedy the human efforts and costs, benefiting automated discovery of architectures in a given search space [8], [9], [10], [11], [12], [13], [14], [15], [16].

Despite the principled automation, NAS still suffers from heavy consumption of computation time and resources. Most NAS methods mainly leverage the validation set and conduct accuracy-driven architecture optimization. Therefore, frequent training and evaluation of sampled architectures become a severe bottleneck that hinders both search efficiency and interpretation. A super-network is extremely slow to be trained till converge [17] with even many effective heuristics

for channel approximations or architecture sampling [18], [19]. Approximated proxy inference such as truncated training/early stopping can accelerate the search, but is observed to introduce severe search bias [10], [20], [21].

People recently address this problem by proposing training-free NAS. Indicators like covariance of sample-wise Jacobian [1], Neural Tangent Kernel [2], and “synflow” [3] are found to highly correlate with network’s accuracy even at initialization (i.e., no gradient descent). This significantly reduces the search cost. However, these works only validated a few highly customized search approaches, and leveraged limited properties of deep networks in an empirical or ad-hoc way. Mellor et al. [1] only considered the “local linear map” defined by the covariance of sample-wise Jacobian, and only studied the random search method. Abdelfattah et al. [3] mainly leveraged “synflow” proposed by previous pruning literature [22] while relying on a warm-up stage. Chen et al. [2] considered two aspects (trainability and expressivity) and integrated two indicators, but still have to leverage highly customized supernet pruning method and cannot extend to other non-supernet NAS search methods. Moreover, these training-free indicators still only pursue final search performance, and we can hardly benefit more about interpretation and understanding of the search trajectory and different search spaces.

In contrast, we target on designing a **unified** and **explainable** training-free NAS framework that is (i) “**search method agnostic**”, i.e., can be scaled up to a broad variety of popular search algorithms; (ii) “**interpretable**”, i.e., can help understand search behaviors on different landscapes of architecture spaces. We first propose to disentangle the network’s characteristics into three distinct aspects: *Trainability*,

- Wuyang Chen, Xinyu Gong, and Zhangyang Wang are with the Department of Electrical and Computer Engineering, The University of Texas at Austin, TX, 78712. E-mail: {wuyang.chen, xinyu.gong, atlaswang}@utexas.edu
- Yunchao Wei is with the Centre for Artificial Intelligence, University of Technology Sydney. E-mail: yunchao.wei@uts.edu.au
- Humphrey Shi is with the Department of Computer and Information Science, University of Oregon. E-mail: hshi3@uoregon.edu
- Zhicheng Yan is with the Facebook AI Applied Research. E-mail: zyan3@fb.com
- Yi Yang is with the Department of Engineering and Information Technology, University of Technology Sydney. E-mail: yi.yang@uts.edu.au
- The first two authors Wuyang Chen and Xinyu Gong contributed equally to this work.
- Correspondence to Zhangyang Wang (atlaswang@utexas.edu).
- The first two authors Wuyang Chen and Xinyu Gong contributed equally to this work.

Expressivity, Generalization, or “TEG” for short. All three could be assessed with training-free indicators, and our studies demonstrate their strong correlations with network’s training or test accuracy. Further, across various network operator types and topologies, they show complementary preferences, together leading to a comprehensive picture. Extensive studies validate the effective and efficient guidance from our TEG-NAS framework, with both improvements on search accuracy and over $2.3\times$ reduction on search time cost. More importantly, we for the first time visualize the search trajectory on architecture landscapes from different search spaces, thanks to our proposed TEG dimensions that disentangles different aspects of the searched model performance and can be efficiently quantified. For example, we find that a good local optimum is easier to find on NAS-Bench-201 [23] which has simpler topologies. However, it is much harder for a search method to balance TEG properties on the DARTS space with complex architecture landscapes. We summarize our contributions as:

- We perform a rigorous correlation analysis of three disentangled “TEG” properties against network’s training and test accuracy, and how changes made to an architecture will affect these aspects. All three notions are measured in a training-free manner. Since the three properties are complementary, they can achieve a very high correlation with the network’s performance if properly combined.
- We design a unified training-free framework to provide accurate yet extremely efficient guidance during NAS search. Our framework is generally applicable to various existing NAS methods, including both supernet and single-path approaches, in a plug-and-play fashion. In both NAS-Bench-201 and DARTS search spaces, we trim down the search time by over $2.3\times$ while improving the searched model’s accuracy.
- Beyond the final search performance, we for the first time visualize the search trajectory on the architecture landscapes from different search spaces, on how the search progresses along the TEG dimensions. That leads to a novel interpretability study of the NAS search process, as well as insightful comparison among different search spaces,

The rest of the paper is organized as follows. After reviewing recent advanced methods for efficient NAS and topics in Deep Learning theory (Section 2), in Section 3 we first introduce our motivation and background in analyzing trainability/expressivity/generalization of deep networks. Definitions and architecture inductive biases of three theory-grounded metrics will be explained, and we will demonstrate that disentangling different aspects of neural architectures leads to a better ranking prediction of networks from a search space. After validating different preferences of our three training-free metrics on network architectures, in Section 4.2 we propose a unified and interpretable NAS framework that does not require any gradient descent training. Our NAS framework can not only be easily integrated into recent popular NAS methods (reinforcement learning, evolution, supernet), but also reflect a novel visualization of architecture landscapes. This contributes to both accelerated high-performance NAS methods and interpretable tools for analyzing NAS search space. We show our final results in Section 5, where we studied the search accuracy and time

cost on both NAS-Bench-201 [23] and DARTS space.

The preliminary version of this work has been published in [2], and we have made significant improvements over it. First, in the main method section, we will introduce a missing part in our ICLR version – a training-free indicator for the generalization (Sec. 3.3). As generalization is a different property of deep networks besides trainability and expressivity, we will demonstrate its strong indication of network performance, its distinct architecture preference (Sec. 4.1), and its contribution to the final search results. Second, this version of training-free NAS is no longer a highly customized algorithm, but a unified and generally adoptable framework, which will be verified in three popular NAS search methods in our experiments (Sec. 5). All three NAS methods will benefit from strong search guidance and significant time cost reduction after being integrated with our general framework. Finally, our new work will facilitate search space visualization and contribute to a novel interpretability study of the NAS search process. By tracking and projecting the search trajectory along the three proposed TEG dimensions, we can observe distinct landscape patterns from simple to complex search spaces, which will provide insights for understanding and designing NAS search spaces.

2 RELATED WORKS

2.1 Neural Architecture Search

Most NAS works suffer from heavy search costs. Sampling-based methods [10], [24], [25], [26] achieve accurate network evaluations, but the truncated training imposes bias on the architecture rankings. The one-shot super network [17], [19], [27], [28] can share parameters to sub-networks and greatly accelerate the evaluations, but it is hard to optimize [29] and suffers from poor correlation between supernet accuracy and its sub-networks’ [30]. In all, there is no clear one-winner method across the variety.

2.2 Efficient and Training-free NAS

Recent NAS works start focusing on reduced training or even training-free search. EcoNAS [31] investigated different ad-hoc proxies (input size, model size, training samples, epochs, etc.) to reduce the training cost. Mellor et al. [1] for the first time proposed a training-free NAS framework, which empirically leverages the correlation between sample-wise Jacobian to rank architectures. However, why did the Jacobian work was not clearly explained and demonstrated. Abdelfattah et al. [3] studied different training-free indicators, and leveraged “synflow” from pruning [22] as the main ranking metric. Chen et al. [2] studied two theory-inspired indicators and combined with supernet pruning for further efficiency. However, these methods either leveraged ad-hoc or limited theory-driven properties of deep networks, or the benefits of their training-free strategies are tied to some specific search methods. In contrast, we hope to explore a comprehensive set of deep network properties, and further propose a unified training-free framework for various existing NAS methods.

2.3 Trainability, Expressivity, and Generalization

Numerous indicators in the deep learning theory field have been proposed to study various aspects of deep networks. Neural tangent kernel (NTK) is proposed to characterize the gradient descent training dynamics of wide networks [32], [33]. It was also proved that wide networks evolve as linear models under gradient descent [34]. Xiao et al. [35] further propose to decouple the network's trainability and generalization. Meanwhile, a network's expressivity can be measured as the number of linear regions separated in the input space [36], [37], [38], [39]. Many works also try directly probe network's generalization from various training statistics or network parameters [40], [41], [42].

3 DISENTANGLING TRAINABILITY, EXPRESSIVITY, AND GENERALIZATION OF DEEP NETWORKS

Trainability, expressivity, and generalization are three important, distinct, and complementary properties to characterize and understand neural networks [35], [38], [40]. Typically, a deep network achieves high performance when: 1) it can produce a loss landscape that is easily trainable with gradient descent, 2) it can represent sufficiently complex functions, 3) it can learn representation transferable to unseen examples, instead of just memorizing training data.

3.1 Trainability

Training deep networks requires optimizing high-dimensional non-convex loss functions. In practice, gradient descent often finds the global or good local minimum. However, many expressible networks are not easily learnable. For example, a deep stack of convolutional layers (e.g. Vgg [4]) is much harder to train than networks with skip connections (ResNet [6], DenseNet [43], etc.), even the former could equip a larger number of parameters. The trainability of a neural network studies how effective it can be optimized by gradient descent [44], [45], [46].

Architecture Bias on Trainability: A network's architecture can control how effectively the gradient information can flow through it. These topological properties might control the amount of information that can be learned by networks. Preserving the gradient flow is found to be essential during network pruning, even at initialization [22], [47]. Skip connections also have a significant impact on the sharpness/flatness of the loss landscapes [48]. Therefore, we hypothesize that certain aspects of trainability can be characterized just by the architecture at its initialization.

Conditioning of NTK: To characterize the training dynamics of wide networks, Neural tangent kernel (NTK) is proposed [34], [49], [50], defined as:

$$\hat{\Theta}(\mathbf{x}, \mathbf{x}') = J(\mathbf{x})J(\mathbf{x}')^T, \quad (1)$$

where $J(\mathbf{x})$ is the Jacobian evaluated at a point \mathbf{x} . Xiao et al. [35] measures the trainability of networks by studying the spectrum and conditioning of $\hat{\Theta}$:

$$\mu_t(\mathbf{x}_{\text{train}}) = (\mathbf{I} - e^{-\eta\hat{\Theta}(\mathbf{x}_{\text{train}}, \mathbf{x}_{\text{train}})^t})\mathbf{y}_{\text{train}} \quad (2)$$

$$\mu_t(\mathbf{x}_{\text{train}})_i = (\mathbf{I} - e^{-\eta\lambda_i t})\mathbf{y}_{\text{train},i}. \quad (3)$$

$\mu_t(\mathbf{x})$ is the expected outputs of a wide network, λ_i are the eigenvalues of $\hat{\Theta}(\mathbf{x}_{\text{train}}, \mathbf{x}_{\text{train}})$, $\mathbf{x}_{\text{train}}$ and $\mathbf{y}_{\text{train}}$ are drawn from the training set D_{train} . Eq. 3 indicates that different

time is needed to learn the i -th eigenmode, and thus we can conclude that the more diverse the learning speeds of different eigenmodes are, the more difficult the network can be optimized. We are therefore motivated to use the empirical condition number of NTK to represent trainability:

$$\hat{\kappa} = \mathbb{E}_{\substack{\mathbf{x}_{\text{train}} \sim D_{\text{train}} \\ \theta \sim \mathcal{N}(0, \frac{2}{N_l})}} \frac{\lambda_{\max}(\hat{\Theta}(\mathbf{x}_{\text{train}}, \mathbf{x}_{\text{train}}))}{\lambda_{\min}(\hat{\Theta}(\mathbf{x}_{\text{train}}, \mathbf{x}_{\text{train}}))}, \quad (4)$$

where network parameters θ are drawn from Kaiming normal initialization $\mathcal{N}(0, \frac{2}{N_l})$ (N_l is the width at layer l) [51], and thus $\hat{\kappa}$ is calculated at network's initialization. As shown in Figure 1, $\hat{\kappa}$ is negatively correlated with both the network's training and test accuracy, with the Kendall-tau correlation as -0.59 . Therefore, minimizing the $\hat{\kappa}$ during the search will encourage the discovery of architectures with high performance.

3.2 Expressivity

Recent works try to explain the success of deep networks by their ability to approximate complex functions, quantified by various complexity measures [52], [53]. The more expressible the network is, the more efficient it can fit the training data. In the case of ReLU networks that compute piecewise linear functions, the number of distinct linear regions is a natural measure of such expressivity. The composition of ReLU leads the input space partitioned into distinct pieces (i.e. linear regions). Therefore, the density of linear regions serves as a convenient proxy for the complexity of the network [36], [38], [39], [54].

Architecture Bias on Expressivity: It was proved that networks with random Gaussian initialization can embed the training data in a distance-preserving manner [55]. Hanin et al. [54] show that the number of activation patterns for ReLU networks is tightly bounded by the total number of neurons both at initialization and during training, and empirically showed that the number of regions stays roughly constant during training [38]. Therefore, network architecture itself has a strong inductive bias on its expressivity.

Complexity of Linear Regions: We first introduce the definition of activation patterns and see how it is connected to the number of linear regions in input space.

Definition 1 of [39] (Activation Patterns as the Linear Regions) Let \mathcal{N} be a ReLU CNN. An activation pattern of \mathcal{N} is a function \mathbf{P} from the set of neurons to $\{1, -1\}$, i.e., for each neuron z in \mathcal{N} , we have $\mathbf{P}(z) \in \{1, -1\}$. Let θ be a fixed set of parameters (weights and biases) in \mathcal{N} , and \mathbf{P} be an activation pattern. The region corresponding to \mathbf{P} and θ is

$$\mathbf{R}(\mathbf{P}; \theta) := \{\mathbf{x}^0 \in \mathbb{R}^{C \times H \times W} : z(\mathbf{x}^0; \theta) \cdot \mathbf{P}(z) > 0, \forall z \in \mathcal{N}\}, \quad (5)$$

where $z(\mathbf{x}^0; \theta)$ is the pre-activation of a neuron z . Let $R_{\mathcal{N}, \theta}$ denote the number of linear regions of \mathcal{N} at θ , i.e., $R_{\mathcal{N}, \theta} := \#\{\mathbf{R}(\mathbf{P}; \theta) : \mathbf{R}(\mathbf{P}; \theta) \neq \emptyset \text{ for some activation pattern } \mathbf{P}\}$.

Eq. 5 tells us that a linear region in the input space is a set of input data \mathbf{x}^0 that satisfies a certain fixed activation pattern $\mathbf{P}(z)$, and therefore the number of linear regions $R_{\mathcal{N}, \theta}$ measures how many unique activation patterns that can be divided by the network.

Since the input space is recursively partitioned by ReLU as the layers go deeper, and the composition of piecewise

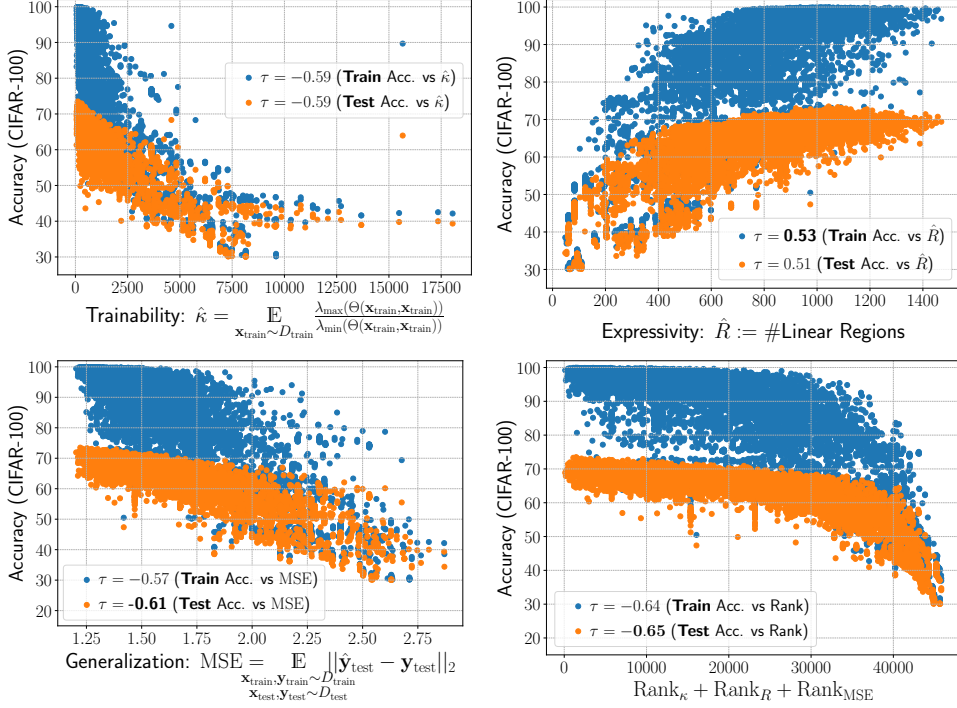


Fig. 1: From left to right: correlation of trainability, expressivity, generalization, and sum of rankings against accuracies in NAS-Bench201 [23], all revealing strong correlations. Meanwhile, expressivity has stronger correlation against training accuracy, and generalization has stronger correlation against test accuracy, which are aligned with their definitions.

linear functions is still piecewise linear, each linear region in the input space can be uniquely represented with a set of affine parameters based on a combination of ReLU activation patterns. This means that, with given training examples and parameters, the number of linear regions $R(\mathbf{x}_{\text{train}}, \theta)$ can be approximated by the number of unique activation patterns combined from all ReLU layers in the whole network. We are therefore motivated to use the empirical number of linear regions to represent expressivity:

$$\hat{R} = \mathbb{E}_{\substack{\mathbf{x}_{\text{train}} \sim D_{\text{train}} \\ \theta \sim \mathcal{N}(0, \frac{2}{L})}} R(\mathbf{x}_{\text{train}}, \theta). \quad (6)$$

As shown in Figure 1, \hat{R} is positively correlated with both the network's training and test accuracy. Moreover, we observe that \hat{R} has a stronger correlation with training over test accuracy, which validates that \hat{R} indicates how well a network fits the training data, but not its generalizability.

3.3 Generalization

Typically, the generalization error is defined as the risk of the model over the underlying data distribution D . A model chosen from a very complex family of functions can essentially fit all the training data, but memorization cannot guarantee the accurate association of unseen examples with seen ones. That makes generalization a distinct notion from trainability ("optimization") and expressivity ("memorization"), since generalization focuses on how well a model can transfer the information from seen to unseen data.

Architecture Bias on Generalization: With even random initialization, network architecture alone could have a strong inductive bias to its generalization error. Network architectures of different complexity or sparsity, without learning any

weight parameters, are found to be able to encode solutions for a given task [56], [57]. Bhardwaj et al. [58] formally established a link between the structure of CNN architectures (depths, widths, number of skip connections, etc.) and their generalization errors. More importantly, inductive bias from certain architecture patterns (e.g. graph-based representation [59]) can even transfer across different types of networks (MLPs, CNNs, ResNets, etc.) and different tasks (CIFAR-10, ImageNet, etc.). Same in our work, we decouple the architecture from the network weights, and focus only on the aspect of "weight-agnostic" generalization, which is impacted by just the network architecture.

NTK Kernel Regression: Previous works [34], [35] showed that at time t during gradient descent training with an MSE loss, the expected outputs of an infinite wide network evolve as:

$$\mu_t(\mathbf{x}_{\text{test}}) = \hat{\Theta}(\mathbf{x}_{\text{test}}, \mathbf{x}_{\text{train}})(\hat{\Theta}(\mathbf{x}_{\text{train}}, \mathbf{x}_{\text{train}}))^{-1}(\mathbf{I} - e^{-\eta \hat{\Theta}(\mathbf{x}_{\text{train}}, \mathbf{x}_{\text{train}})t})\mathbf{y}_{\text{train}}. \quad (7)$$

Studying the evolution of $\mu_t(\mathbf{x}_{\text{test}})$ in Eq. 7 along the training iteration t can characterize the generalization performance of deep networks. However, the infinite width is not directly applicable in real-life scenarios, and we want to estimate the generalization at a network's initialization. Therefore in our work, we choose to empirically estimate the generalization by calculating the test MSE error of a network's NTK kernel regression:

$$\hat{y}_{\text{test}} = \hat{\Theta}^L(\mathbf{x}_{\text{test}}, \mathbf{x}_{\text{train}})(\hat{\Theta}^L(\mathbf{x}_{\text{train}}, \mathbf{x}_{\text{train}}))^{-1}\mathbf{y}_{\text{train}}, \quad (8)$$

$$\text{MSE} = \mathbb{E}_{\substack{\mathbf{x}_{\text{train}}, \mathbf{y}_{\text{train}} \sim D_{\text{train}} \\ \mathbf{x}_{\text{test}}, \mathbf{y}_{\text{test}} \sim D_{\text{test}}}} \|\hat{y}_{\text{test}} - \mathbf{y}_{\text{test}}\|_2. \quad (9)$$

$\hat{\Theta}^L$ indicates the NTK evaluated only for the last layer of the

deep network. Eq. 8 tries to associate x_{test} with x_{train} via NTK kernel regression, and transfer the given training labels y_{train} to the test data. A deep neural network will fail to generalize if its prediction \hat{y}_{test} becomes data-independent, and the MSE in Eq. 9 will become large.

Note that we are not directly predicting a network's converged generalization at its initialization. Instead, we use MSE to compare different networks and study how it would be affected by different architectures. Adopting MSE also follows the convention that NTK is also derived under the squared loss [32], [60]. As further demonstrated in Figure 1, MSE shows strong negative correlation with both the network's training accuracy and test accuracy. More importantly, it has a stronger correlation with the test than the training accuracy. This precisely validates that MSE represents how well a network generalizes, but not memorization of the training data.

At this moment we disentangled the network's performance into three distinct properties. In the next section, we present our unified and interpretable TEG-NAS strategy.

4 TEG-NAS: A UNIFIED AND INTERPRETABLE NAS FRAMEWORK

Our core motivation is to provide a unified training-free framework for NAS of both high performance and low cost. We also enable the interpretability of NAS by visualizing the search trajectory on the architecture landscapes.

4.1 How Architecture Affects $\hat{\kappa}$, \hat{R} , and MSE

Despite the strong correlations and different preferences over training or testing accuracy we observe in Figure 1, it is still unknown whether each individual aspect of three – trainability, expressivity, generalization – is necessary for a deep network to be of high performance. This analysis is also missing in previous works [2], [35]. Before we directly adopt our disentangled TEG properties to NAS search, we must study how changes of $\hat{\kappa}$, \hat{R} , MSE could be reflected on network architectures, and how network's operator types or topology will affect its trainability, expressivity, and generalization. Otherwise, if they share the same preference on selecting architectures, picking any one of them will guide the search towards similar results.

Architecture Exclusively Selected by $\hat{\kappa}$, \hat{R} , MSE

Trainability, expressivity, and generalization may have different preferences over network's operator types and topology. This motivates us to summarize architectures that are exclusively selected by $\hat{\kappa}$, \hat{R} , MSE. We first measure the thresholds T_{κ} , T_R , T_{MSE} that filter top 10% architectures out of the search space \mathbf{A} , ranked by $\hat{\kappa}$, \hat{R} , and MSE, respectively. We define the following three subsets of architectures, with any two out of three having an empty intersection:

$$\mathbf{A}_{\kappa} = \{a | a \in \mathbf{A}, \hat{\kappa}_a \leq T_{\kappa}, \hat{R}_a < T_R, \text{MSE}_a > T_{\text{MSE}}\}, \quad (10)$$

$$\mathbf{A}_R = \{a | a \in \mathbf{A}, \hat{\kappa}_a > T_{\kappa}, \hat{R}_a \geq T_R, \text{MSE}_a > T_{\text{MSE}}\}, \quad (11)$$

$$\mathbf{A}_{\text{MSE}} = \{a | a \in \mathbf{A}, \hat{\kappa}_a > T_{\kappa}, \hat{R}_a < T_R, \text{MSE}_a \leq T_{\text{MSE}}\}. \quad (12)$$

We study three subsets of architectures in terms of both operator and topology, shown in Figure 2. For operator types, the ratio of convolution (1 \times 1 and 3 \times 3) operators in \mathbf{A}_{κ} is lower than those of \mathbf{A}_R and \mathbf{A}_{MSE} , indicating operators

with a heavy number of parameters may not friendly for optimization. In contrast, \mathbf{A}_R and \mathbf{A}_{MSE} favor more convolution layers, benefiting to data fitting. For network topology, the averaged depth¹ of architectures in \mathbf{A}_{κ} is much lower than those in \mathbf{A}_R , since shallow networks are easier to train [35]. Depth from \mathbf{A}_{MSE} is also low, contributing to better test accuracy.

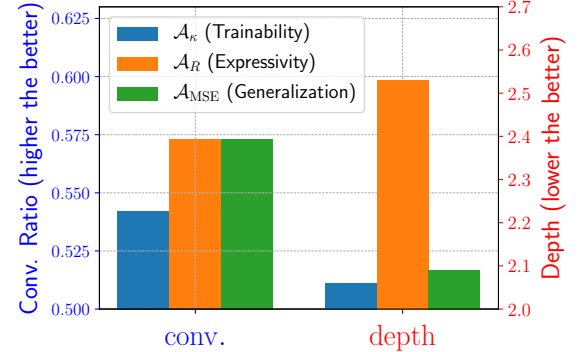


Fig. 2: Impact of network operators and topologies on $\hat{\kappa}$, \hat{R} , and MSE in NAS-Bench201.

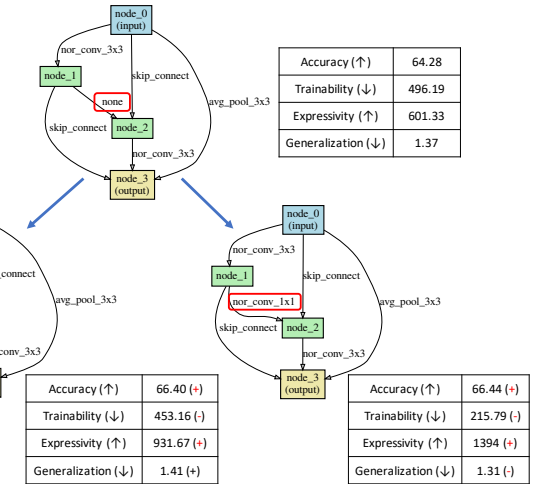


Fig. 3: “None” operator jeopardize the architecture's trainability, expressivity, and generalization. By replacing “none” with “skip_connect” or “conv1 \times 1”, the bad trainability or expressivity can be addressed, leading to better test accuracy.

Case Study

One failure reason for a bad architecture is the exist of “none” (or “zero”) operator, which completely breaks the feed-forward and gradient flow. We show one case in Figure 3. When there is a “none” exist, both trainability and expressivity are bad, leading to poor test accuracy. By switching into “skip_connect” or “conv1 \times 1”, the bad trainability or expressivity are addressed, leading to better test accuracy.

4.2 A Unified Training-free NAS Framework

Different preferences of $\hat{\kappa}$, \hat{R} , and MSE on network's operators and topology validate their potential of guiding the

1. Depth of a cell is defined as the number of connections on the longest path from input to the output [61]

TABLE 1: Comparison of different NAS search methods studied in our experiments.

NAS Method	NAS Formulation	Weight-sharing	Update Method	Search Stopping Criterion
REINFORCE	Single-path	No	policy gradients	policy entropy
Evolution	Single-path	No	mutation	population diversity
FP-NAS	Supernet	Yes	gradient descent	entropy of architecture parameters

NAS search. We now propose our unified training-free NAS framework (Algorithm 1). Existing NAS methods evaluate the accuracy or loss value of every single architecture via truncated training or shared supernet weights. The evaluated accuracy or loss is also leveraged as feedback to update the NAS method itself. Instead, we leverage the disentangled trainability, expressivity, and generalization during the search. For each architecture sampled by the NAS search method, we average three repeated calculations of $\hat{\kappa}_t / \hat{R}_t / \text{MSE}_t$, by using three independent mini-batches of training data. They will be leveraged as the feedback to guide the update of the search method. For different search stopping criteria and update manners of different NAS methods, please refer to Section 5.1, Table 1, and also our supplement for implementation details.

Algorithm 1 Our unified training-free framework for different NAS methods.

```

1: Input: architecture search space  $\mathcal{A}$ , NAS search method  $\mathcal{M}$ , step  $t = 0$ .
2: while not Search Stopping Criterion of  $\mathcal{M}$  satisfied do
3:   Sample architecture:  $a_t = \mathcal{M}.\text{sample}(\mathcal{A})$ 
4:   Calculate  $\hat{\kappa}_t$ ,  $\hat{R}_t$ ,  $\text{MSE}_t$  for  $a_t$ 
5:   Update NAS method:  $\mathcal{M}.\text{update}(a_t, \hat{\kappa}_t, \hat{R}_t, \text{MSE}_t)$ 
6:    $t = t + 1$ 
7: end while
8: Return Searched architecture  $\mathcal{M}.\text{derive}()$ .
```

Comparison with Prior Works

- Mellor et al. [1] only leveraged sample-wise correlation of Jacobian, with no detailed explanation of which aspect (trainability/expressivity/generalization) this metric represents. Moreover, they only leveraged Random Search on NAS-Bench-201, without studying more NAS methods and search spaces.
- Abdelfattah et al. [3] mainly leveraged “synflow” metric equipped with “warm-up” or “move proposal” search strategy, which is related to trainability. However, they still have to use trained models for proxy inference during the search.
- Chen et al. [2] built their framework on top of a super-net based approach, and strongly rely on a highly customized super-net pruning strategy. We evaluate their method without pruning (shown in Table 2) and observed inferior performance.

4.3 Visualizing Search Process on Different Architecture Landscapes

It has been a missing part in the NAS community to visualize the search process on architecture landscapes from different search spaces. Several bottlenecks hinder this analysis: 1) evaluation via truncated training still suffers from heavy computation cost, making the architecture landscape intractable

to characterize; 2) the truncated accuracy or loss value is noisy, making the trade-off of exploration-exploitation of the search process hard to observe.

We leverage the Reinforcement Learning as the example, and take pioneering steps to conduct such analysis:

- To explore the global and local geometry of the architecture landscapes, at search step t we spawn a parent architecture into two children, and proceed the search of these two children with different randomness.
- We collect the trajectory of architectures from two children, and project the high-dimensional architecture space into a 2D plane via PCA.

We perform these analysis at early and late search steps on both NAS-Bench-201 space [23] and DARTS search space [17] (see search space details in Section 5), shown in Figure 4. Our observations are summarized as follows:

- On NAS-Bench-201, the search can land in areas where $\hat{\kappa}_t$, \hat{R}_t , and MSE_t are all good. Although some areas (e.g. area “A” in early NAS-Bench-201) enjoy local minimal on one of the three aspects, the search will proceed beyond it due to its inferiority on the other two properties.
- Spawning at both early and late search stage, two children from NAS-Bench-201 land in the same area in the end. This is probably because of the simple operator types and topology from the design of NAS-Bench-201 (see details in Section 5.3 and original paper [23]).
- DARTS space is associated with much more complex architecture landscapes. Children spawned from both early and late stage may land in different areas, with a barrier (or a valley) on their interpolation (orange dashed line). This complex landscape introduce significant challenge to balance and trade-off $\hat{\kappa}_t$, \hat{R}_t , and MSE_t for NAS search, with even noisy signals.

The impact of our landscape analysis lies in two folds:

- 1) For designing **NAS algorithms**: visualizing the search process can reveal the quality and stability of the search via different spawning and randomness.
- 2) For designing **search spaces**: [62], [63], visualizing the architecture landscapes can help study the complexity and geometry of the search space.

5 EXPERIMENTS

In this section, we evaluate our TEG-NAS framework on two search spaces: NAS-Bench-201 [23] and DARTS [17]. Training protocols are summarized in our supplement. For DARTS space, we conduct experiments on both CIFAR-10 and ImageNet (Section 5.4). For NAS-Bench-201, we test all three supported datasets (CIFAR-10, CIFAR-100, ImageNet-16-120 [67]) in section 5.3.

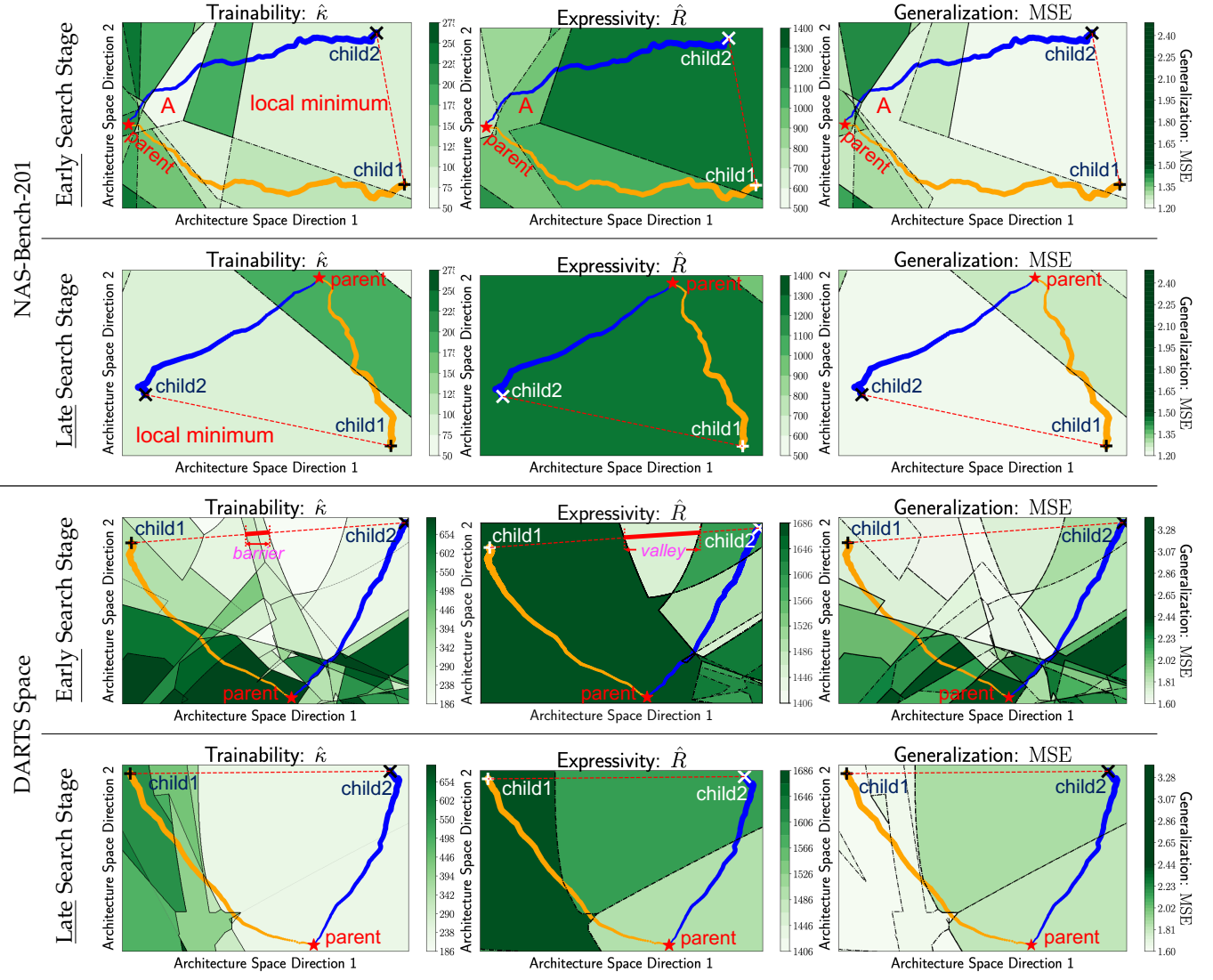


Fig. 4: The architecture landscape with respect to trainability (left), expressivity (middle), and generalization (right) on a 2D plane projected via PCA from the search space. The red star indicates the parent of a search by Reinforcement Learning, and two crosses represent two children spawned from the same parent (at “Early” or “Late” search stage), but searched with different randomness. The simple geometry of NAS-Bench-201 is easier to search, whereas the DARTS space is much more complex and hard to explore.

5.1 Studied Search Methods

REINFORCE [10], [64]: Reinforcement learning (RL) treats the NAS search process as a sequential decision making process. The policy agent formulates a single-path architecture by choosing a sequence of operators as actions, and uses the accuracy, loss value, or our training-free indicators of sampled architecture as the reward to update its internal policy distribution.

Evolution [24]: Starting from a randomly initialized pool of architectures, the evolution keeps updating the population by mutating the high-ranked architectures. The ranking criteria could be the accuracy, loss value, or our training-free indicators of sampled architectures.

Fast Probabilistic NAS: FP-NAS views search evaluations from an underlying distribution over architectures [65]. It constructs a supernet and corresponding architecture parameters. Leveraging Importance Weighted Monte-Carlo EB algorithm [68], architecture parameters are optimized to

maximize the model likelihoods of sampled architectures, which are weighted by a proxy architecture performance indicator, like accuracy, loss value, or training-free indicators.

5.2 Implementation Details

In this section, we include more details regarding Algorithm 1 in terms of different search methods.

5.2.1 Reinforcement Learning

The policy agent maintains a internal state to represent the architecture search space, denoted as θ^A . This internal state can be converted to a categorical distribution of the architectures (\mathcal{A}) via softmax: $\mathcal{A} = \sigma(\theta^A)$.

Stopping Criterion: We stop the RL search when the entropy of \mathcal{A} stops decreasing (total iterations $T = 500$ in our work). We train the RL agent with a learning rate as $\eta = 0.04$ on NAS-Bench-201 and $\eta = 0.07$ on DARTS space.

TABLE 2: Search Performance from NAS-Bench-201. Test accuracy with mean and deviation are reported. “optimal” indicates the best test accuracy achievable in the space. The search time cost of our TEG-NAS is agnostic to the size of dataset (Section 4.2). For REINFORCE [64], Evolution [24], and FP-NAS [65], three search costs are listed for CIFAR-10/CIFAR-100/ImageNet-16-120.

Architecture	CIFAR-10	CIFAR-100	ImageNet-16-120	Search Cost (GPU sec.)	Search Method
ResNet [6]	93.97	70.86	43.63	-	-
RSPS [66]	87.66(1.69)	58.33(4.34)	31.14(3.88)	8007.13	random
ENAS [10]	54.30(0.00)	15.61(0.00)	16.32(0.00)	13314.51	RL
DARTS (1st) [17]	54.30(0.00)	15.61(0.00)	16.32(0.00)	10889.87	gradient
DARTS (2nd) [17]	54.30(0.00)	15.61(0.00)	16.32(0.00)	29901.67	gradient
GDAS [19]	93.61(0.09)	70.70(0.30)	41.84(0.90)	28925.91	gradient
NAS w.o. Training [1]	91.78(1.45)	67.05(2.89)	37.07(6.39)	4.8	training-free
TE-NAS [2]	93.9(0.47)	71.24(0.56)	42.38(0.46)	1558	training-free
TE-NAS + TEG (ours)	93.94(0.2)	71.44(0.81)	44.11(0.88)	3330.5	training-free
REINFORCE [64]	90.00(1.16)	68.40(5.93)	44.78(1.20)	33.9k/35.9k/63.5k	RL
REINFORCE + TEG (ours)	90.21(0.67)	70.42(0.36)	44.88(0.91)	3668.5	training-free
Evolution [24]	90.92(0.31)	69.32(3.31)	44.33(1.81)	33.7k/38.1k/148.3k	evolution
Evolution + TEG (ours)	91.00(0.33)	70.10(1.47)	44.45(0.75)	9939.5	training-free
FP-NAS [65]	55.38(1.52)	22.30(15.45)	16.96(6.43)	3.7k/6.6k/17.2k	gradient
FP-NAS + TEG (ours)	93.73(0.50)	70.36(0.44)	46.03(0.10)	641.67	training-free
Optimal	94.37	73.51	47.31	-	-

Architecture Sampling: In each iteration, the agent samples one architecture a_t from \mathcal{A} .

Update: We update the RL agent via policy gradients.

$$\theta_{t+1}^A = \theta_t^A - \eta \cdot \nabla_{\theta^A} f(\theta_t^A) \quad t = 1, \dots, T \quad (13)$$

$$f(\theta_t^A) = -\log(\sigma(\theta^A)) \cdot (r_t - b_t) \quad (14)$$

$$b_t = \gamma b_{t-1} + (1 - \gamma)r_t \quad (b_0 = 0, \gamma = 0.9) \quad (15)$$

r stands for reward, and b for an exponential moving average of reward for the purpose of variance reduction. For the baseline method, reward is taken from the proxy inference, i.e., the test accuracy by 1-epoch truncated training. For our TEG-NAS, reward is composed of three parts: $r = r^\kappa + r^R + r^{\text{MSE}}$. Taking r^κ (reward from trainability) as the example:

$$r_t^\kappa = \frac{\hat{\kappa}_t - \hat{\kappa}_{t-1}}{\hat{\kappa}_{\max,t} - \hat{\kappa}_{\min,t}} \quad (16)$$

$$\hat{\kappa}_{\max,t} = \max(\hat{\kappa}_1, \hat{\kappa}_2, \dots, \hat{\kappa}_t) \quad (17)$$

$$\hat{\kappa}_{\min,t} = \min(\hat{\kappa}_1, \hat{\kappa}_2, \dots, \hat{\kappa}_t) \quad (18)$$

where $\hat{\kappa}_t$ is the evaluated trainability of the architecture sampled at step t . We calculate r^R (expressivity) and r^{MSE} (generalization) in the same way.

Architecture Deriving: To derive the final searched network, the agent chooses the architecture that has the highest probability, i.e., $a^* = \text{argmax}_a \sigma(\theta^A)(a)$.

5.2.2 Evolution

The evolution search is first initialized with a population of 256 architectures by random sampling. We choose the size of the population based on Figure A-1(a) from [24].

Stopping Criterion: We stop the Evolution search when the population diversity stops decreasing (1000 iterations in our work). Population diversity is calculated as the averaged pair-wise architecture difference in their operator types.

Architecture Sampling: Following Real et al. [24], in each iteration, the evolution search first randomly samples a

subset of 64 architectures out of the population. We choose this sampling size based on Figure A-1(a) from [24]. Next, the best architecture (a_t) from this subset is selected. For the baseline method, the best architecture is the top1 ranked by the proxy inference, i.e., the test accuracy by 1-epoch truncated training. For our TEG-NAS, the best architecture is the top1 by the sum of three rankings by trainability, expressivity, and generalization: $\text{rank}^\kappa + \text{rank}^R + \text{rank}^{\text{MSE}}$. Each rank is calculated by sorting architectures in this current subset.

Update: Following Real et al. [24], in each iteration the population is updated by adding a new architecture and popping out the oldest architecture (the one that stays in the population for the longest time). The new architecture is generated by mutating the sampled one mentioned above. We follow the same mutation strategy from Real et al. [24].

Architecture Deriving: To derive the final searched network, the best architecture from the population is selected, where the criterion is the same as we choose a_t (see above “Architecture Sampling”).

5.2.3 Fast Probabilistic NAS

The Fast Probabilistic NAS (FP-NAS) formulates the search space as a supernet and shares its parameters to its subnetworks. The original FP-NAS search performs alternative optimization between network parameters and the architecture parameters (denoted as θ^A). This architecture parameter can be converted to a categorical distribution of the architectures (\mathcal{A}) via softmax: $\mathcal{A} = \sigma(\theta^A)$.

Stopping Criterion: We stop the FP-NAS search when the entropy of \mathcal{A} stops decreasing (total epochs $T = 100$ in our work). We update the architecture parameters with a learning rate as $\eta = 0.1$.

Architecture Sampling: In each step, the FP-NAS samples a subset A_t of $\lambda H(\text{Prob}(a_i|\mathcal{A}))$ architectures from \mathcal{A} . Here H denotes the distribution entropy and λ is a pre-defined scaling factor where we set it to 0.25.

TABLE 3: Search Performance from DARTS space on CIFAR-10.

Architecture	Test Error (%)	Params (M)	Search Cost (GPU days)	Search Method
AmoebaNet-A [24]	3.34	3.2	3150	evolution
PNAS [11] [*]	3.41	3.2	225	SMBO
ENAS [10]	2.89	4.6	0.5	RL
NASNet-A [69]	2.65	3.3	2000	RL
DARTS (1st) [17]	3.00	3.3	0.4	gradient
SNAS [70]	2.85	2.8	1.5	gradient
GDAS [19]	2.82	2.5	0.17	gradient
BayesNAS [71]	2.81	3.4	0.2	gradient
ProxylessNAS [72] [†]	2.08	5.7	4.0	gradient
P-DARTS [73]	2.50	3.4	0.3	gradient
PC-DARTS [18]	2.57	3.6	0.1	gradient
SDARTS-ADV [74]	2.61	3.3	1.3	gradient
TE-NAS [2]	2.63	3.8	0.05 [‡]	training-free
REINFORCE [64]	3.01	2.3	1.1 [‡]	RL
REINFORCE + TEG (ours)	2.91	3.6	0.15 [‡]	training-free
Evolution [24]	3.01	2.1	2.6 [‡]	evolution
Evolution + TEG (ours)	2.75	4.0	0.4 [‡]	training-free
FP-NAS [65]	5.38	2.02	0.3 [‡]	gradient
FP-NAS + TEG (ours)	2.66	4.42	0.13 [‡]	training-free

^{*} No cutout augmentation.

[†] Different space: PyramidNet [75] as the backbone.

[‡] Recorded on a single GTX 1080Ti GPU.

Update: We update the architecture parameters by stochastic gradient descent.

$$\theta_{t+1}^A = \theta_t^A - \eta \cdot \nabla_{\theta^A} f(\theta_t^A) \quad t = 1, \dots, T \quad (19)$$

$$f(\theta_t^A) = - \sum_{i=1}^{|A_t|} \log(\text{Prob}(a_i | A)) \cdot \frac{e^{r_i}}{\sum_{j=1}^{|A_t|} e^{r_j}} \quad (20)$$

r stands for reward, calculated in the same way as we did for Reinforcement Learning (Section 5.2.1).

Architecture Deriving: To derive the final searched network, the FP-NAS chooses the architecture that has the highest probability, i.e., $a^* = \text{argmax}_a \sigma(\theta^A)(a)$.

5.3 Results on NAS-Bench-201

NAS-Bench-201 [23] provides a cell-based search space and the performance of all 15,625 networks it contains using a unified protocol. The network's accuracy is directly available by querying the database, benefiting towards the study of NAS methods without network evaluation. It contains five operator types: *none (zero)*, *skip connection*, *separable convolution* 3×3 and 5×5 , *dilated separable convolution* 3×3 and 5×5 , *max pooling* 3×3 , *average pooling* 3×3 . We refer to their paper for details of the space. For the baseline methods, the RL agent and Evolution use the test accuracy after 1-epoch training as the reward or ranking criteria. The FP-NAS uses alternative training between architecture parameters and supernet parameters with stochastic gradient descent. For all results we report, we run for four independent times with different random seeds, and report the mean and standard deviation in Table 2.

We can see that for all three NAS methods (REINFORCE, Evolution, FP-NAS), our TEG-NAS framework boosts the

search performance while significantly reduce the search time cost. Although [1] costs reduced search time (sampled only 25 architectures), they suffer from much inferior search accuracy and significantly larger variance. Moreover, by adopting our unified framework, the accuracy of TE-NAS can be further improved.

5.4 Results on DARTS Search Space

Architecture Space The DARTS space contains eight operator types: *none (zero)*, *skip connection*, *separable convolution* 3×3 and 5×5 , *dilated separable convolution* 3×3 and 5×5 , *max pooling* 3×3 , *average pooling* 3×3 . During the evaluation we stack 20 cells to compose the network and set the initial channel number as 36 [17], [18], [73]. We place the reduction cells at the 1/3 and 2/3 of the network. Each cell contains six nodes.

The architecture for ImageNet is slightly different: the network is stacked with 14 cells with the initial channel number set to 48. During retraining evaluation. The spatial resolution is downsampled from 224×224 to 28×28 with the first three convolution layers of stride 2.

Evaluation Protocols We follow previous NAS works [18], [73], [74] to evaluate architectures after search. On CIFAR-10, we train the searched network with cutout regularization of length 16, drop-path [69] with probability as 0.3, and an auxiliary tower of weight 0.4. On ImageNet, we also use label smoothing during training. On both CIFAR-10 and ImageNet, the network is optimized by an SGD optimizer with cosine annealing, with a learning rate initialized as 0.025 and 0.5, respectively.

TABLE 4: Search Performance from DARTS space on ImageNet.

Architecture	Test Error(%)		Params (M)	Search Cost (GPU days)	Search Method
	top-1	top-5			
NASNet-A [69]	26.0	8.4	5.3	2000	RL
AmoebaNet-C [24]	24.3	7.6	6.4	3150	evolution
PNAS [11]	25.8	8.1	5.1	225	SMBO
MnasNet-92 [76]	25.2	8.0	4.4	-	RL
DARTS (2nd) [17]	26.7	8.7	4.7	4.0	gradient
SNAS (mild) [70]	27.3	9.2	4.3	1.5	gradient
GDAS [19]	26.0	8.5	5.3	0.21	gradient
BayesNAS [71]	26.5	8.9	3.9	0.2	gradient
P-DARTS (CIFAR-10) [73]	24.4	7.4	4.9	0.3	gradient
P-DARTS (CIFAR-100) [73]	24.7	7.5	5.1	0.3	gradient
PC-DARTS (CIFAR-10) [18]	25.1	7.8	5.3	0.1	gradient
ProxylessNAS (GPU) [72] [†]	24.9	7.5	7.1	8.3	gradient
PC-DARTS (ImageNet) [18] [†]	24.2	7.3	5.3	3.8	gradient
TE-NAS [2]	26.2	8.3	6.3	0.05	training-free
REINFORCE [64]	27.8	9.3	3.6	1.1	RL
REINFORCE + TEG (ours)	25.0	7.3	5.1	0.15	training-free
Evolution [24]	28.8	10	3.3	2.6	evolution
Evolution + TEG (ours)	26.3	8.4	5.6	0.4	training-free
FP-NAS [65]	32.6	12.3	3.3	0.3	gradient
FP-NAS + TEG (ours)	23.4	7.0	5.9	0.13	training-free

[†] Architecture searched on ImageNet, otherwise searched on CIFAR-10 or CIFAR-100.

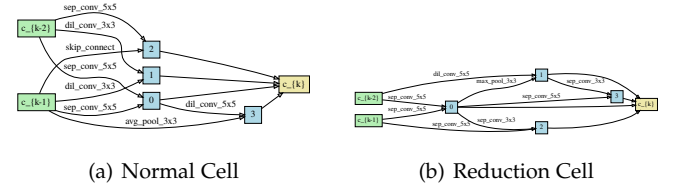
Results Table 3 and 4 summarize the performance on CIFAR-10 and ImageNet. On three different NAS methods and two datasets, our training-free framework can reduce the top1 error and further save the search time cost over $2.3\times$. FP-NAS equipped with our TEG framework can even achieve the best top1 error evaluated on ImageNet. All training-free versions of three NAS methods can now complete the search with less than a half GPU day. These search improvements on the large-scale DARTS space and datasets validate the effectiveness and efficiency of our unified TEG-NAS framework.

5.5 Searched Architecture on DARTS Search Space

We visualize the searched normal and reduction cells on DARTS space, by Reinforcement Learning (Figure 5), Evolution (Figure 6), and FP-NAS (Figure 7).

TABLE 5: Ablation study of different combinations of training-free indicators for REINFORCE NAS method on NAS-Bench-201 CIFAR-100. Test accuracy with mean and deviation are reported.

Indicators	Accuracy	GPU secs.
Baseline (1-epoch training)	68.4(5.93)	19786
\hat{R}	69.06(2.15)	254.6
$\hat{\kappa}$	69.27(0.73)	1574
MSE	69.68(0.88)	2447.7
$\hat{\kappa}, \hat{R}$	69.89(0.98)	1716.1
\hat{R}, MSE	70.00(0.42)	2667.4
$\hat{\kappa}, \text{MSE}$	70.18(0.04)	2704
$\hat{\kappa}, \hat{R}, \text{MSE}$	70.42(0.36)	3668.5



study in Table 5 using Reinforcement Learning on Cifar100 on NAS-Bench-201. As the baseline method, the RL agent uses the test accuracy after 1-epoch training as the reward. We can see that the guidance from every single indicator outperforms the truncated training, with much less search time cost. Finally, we achieve the best search performance once equipped with all $\hat{\kappa}$, \hat{R} , and MSE.

6 CONCLUSION

We proposed a **unified** and **explainable** NAS framework that benefit both various popular search methods and search interpretation. We successfully disentangle the network's characteristics into three distinct aspects: *Trainability*, *Expressivity*, *Generalization*, or "TEG" for short, and leverage all of them to provide effective and efficient guidance for NAS search. Extensive studies on different NAS search methods validate the superior performance of our TEG-NAS framework. More importantly, we for the first time visualize the search trajectory on architecture landscapes from different search spaces, contributing to a better understanding of both search and geometry of architecture space. We hope our work encourages the community to further explore NAS methods that benefit from extremely low cost, and provide a better understanding of the architectures and complexity of different search spaces.

REFERENCES

- [1] J. Mellor, J. Turner, A. Storkey, and E. J. Crowley, "Neural architecture search without training," *arXiv preprint arXiv:2006.04647*, 2020.
- [2] W. Chen, X. Gong, and Z. Wang, "Neural architecture search on imagenet in four gpu hours: A theoretically inspired perspective," in *International Conference on Learning Representations*, 2021.
- [3] M. Abdelfattah, A. Mehrotra, L. Dudziak, and D. N. Lane, "Zero-cost proxies for lightweight nas," in *International Conference on Learning Representations*, 2021.
- [4] K. Simonyan and A. Zisserman, "Very deep convolutional networks for large-scale image recognition," *arXiv preprint arXiv:1409.1556*, 2014.
- [5] C. Szegedy, W. Liu, Y. Jia, P. Sermanet, S. Reed, D. Anguelov, D. Erhan, V. Vanhoucke, and A. Rabinovich, "Going deeper with convolutions," in *Proceedings of the IEEE conference on computer vision and pattern recognition*, 2015, pp. 1–9.
- [6] K. He, X. Zhang, S. Ren, and J. Sun, "Deep residual learning for image recognition," in *Proceedings of the IEEE conference on computer vision and pattern recognition*, 2016, pp. 770–778.
- [7] S. Xie, R. Girshick, P. Dollár, Z. Tu, and K. He, "Aggregated residual transformations for deep neural networks," in *Proceedings of the IEEE conference on computer vision and pattern recognition*, 2017, pp. 1492–1500.
- [8] B. Zoph and Q. V. Le, "Neural architecture search with reinforcement learning," *arXiv preprint arXiv:1611.01578*, 2016.
- [9] A. Brock, T. Lim, J. M. Ritchie, and N. Weston, "Smash: one-shot model architecture search through hypernetworks," *arXiv preprint arXiv:1708.05344*, 2017.
- [10] H. Pham, M. Y. Guan, B. Zoph, Q. V. Le, and J. Dean, "Efficient neural architecture search via parameter sharing," *arXiv preprint arXiv:1802.03268*, 2018.
- [11] C. Liu, B. Zoph, M. Neumann, J. Shlens, W. Hua, L.-J. Li, L. Fei-Fei, A. Yuille, J. Huang, and K. Murphy, "Progressive neural architecture search," in *Proceedings of the European Conference on Computer Vision (ECCV)*, 2018, pp. 19–34.
- [12] L.-C. Chen, M. Collins, Y. Zhu, G. Papandreou, B. Zoph, F. Schroff, H. Adam, and J. Shlens, "Searching for efficient multi-scale architectures for dense image prediction," in *Advances in Neural Information Processing Systems*, 2018, pp. 8699–8710.
- [13] G. Bender, P.-J. Kindermans, B. Zoph, V. Vasudevan, and Q. Le, "Understanding and simplifying one-shot architecture search," in *International Conference on Machine Learning*, 2018, pp. 549–558.
- [14] X. Gong, S. Chang, Y. Jiang, and Z. Wang, "Autogan: Neural architecture search for generative adversarial networks," in *Proceedings of the IEEE International Conference on Computer Vision*, 2019, pp. 3224–3234.
- [15] Y. Fu, W. Chen, H. Wang, H. Li, Y. Lin, and Z. Wang, "Autogan-distiller: Searching to compress generative adversarial networks," in *International Conference on Machine Learning*. PMLR, 2020, pp. 3292–3303.
- [16] W. Chen, X. Gong, X. Liu, Q. Zhang, Y. Li, and Z. Wang, "Fasterseg: Searching for faster real-time semantic segmentation," in *International Conference on Learning Representations*, 2019.
- [17] H. Liu, K. Simonyan, and Y. Yang, "Darts: Differentiable architecture search," *arXiv preprint arXiv:1806.09055*, 2018.
- [18] Y. Xu, L. Xie, X. Zhang, X. Chen, G.-J. Qi, Q. Tian, and H. Xiong, "Pcdarts: Partial channel connections for memory-efficient architecture search," in *International Conference on Learning Representations*, 2019.
- [19] X. Dong and Y. Yang, "Searching for a robust neural architecture in four gpu hours," in *Proceedings of the IEEE Conference on computer vision and pattern recognition*, 2019, pp. 1761–1770.
- [20] H. Liang, S. Zhang, J. Sun, X. He, W. Huang, K. Zhuang, and Z. Li, "Darts+: Improved differentiable architecture search with early stopping," *arXiv preprint arXiv:1909.06035*, 2019.
- [21] M. Tan, R. Pang, and Q. V. Le, "Efficientdet: Scalable and efficient object detection," in *Proceedings of the IEEE/CVF Conference on Computer Vision and Pattern Recognition*, 2020, pp. 10781–10790.
- [22] H. Tanaka, D. Kunin, D. L. Yamins, and S. Ganguli, "Pruning neural networks without any data by iteratively conserving synaptic flow," *arXiv preprint arXiv:2006.05467*, 2020.
- [23] X. Dong and Y. Yang, "Nas-bench-102: Extending the scope of reproducible neural architecture search," *arXiv preprint arXiv:2001.00326*, 2020.
- [24] E. Real, A. Aggarwal, Y. Huang, and Q. V. Le, "Regularized evolution for image classifier architecture search," in *Proceedings of the aaai conference on artificial intelligence*, vol. 33, 2019, pp. 4780–4789.
- [25] Z. Li, T. Xi, J. Deng, G. Zhang, S. Wen, and R. He, "Gp-nas: Gaussian process based neural architecture search," in *Proceedings of the IEEE/CVF Conference on Computer Vision and Pattern Recognition*, 2020, pp. 11933–11942.
- [26] Z. Yang, Y. Wang, D. Tao, X. Chen, J. Guo, C. Xu, C. Xu, and C. Xu, "Hournas: Extremely fast neural architecture search through an hourglass lens," *arXiv preprint arXiv:2005.14446*, 2020.
- [27] J. Yu, P. Jin, H. Liu, G. Bender, P.-J. Kindermans, M. Tan, T. Huang, X. Song, R. Pang, and Q. Le, "Bignas: Scaling up neural architecture search with big single-stage models," *arXiv preprint arXiv:2003.11142*, 2020.
- [28] G. Li, G. Qian, I. C. Delgadillo, M. Muller, A. Thabet, and B. Ghanem, "Sgas: Sequential greedy architecture search," in *Proceedings of the IEEE/CVF Conference on Computer Vision and Pattern Recognition*, 2020, pp. 1620–1630.
- [29] K. Yu, R. Ranftl, and M. Salzmann, "How to train your super-net: An analysis of training heuristics in weight-sharing nas," *arXiv preprint arXiv:2003.04276*, 2020.
- [30] K. Yu, C. Sciuти, M. Jaggi, C. Musat, and M. Salzmann, "Evaluating the search phase of neural architecture search," in *ICLR*, 2020.
- [31] D. Zhou, X. Zhou, W. Zhang, C. C. Loy, S. Yi, X. Zhang, and W. Ouyang, "Econas: Finding proxies for economical neural architecture search," in *Proceedings of the IEEE/CVF Conference on Computer Vision and Pattern Recognition*, 2020, pp. 11396–11404.
- [32] A. Jacot, F. Gabriel, and C. Hongler, "Neural tangent kernel: Convergence and generalization in neural networks," in *Advances in neural information processing systems*, 2018, pp. 8571–8580.
- [33] B. Hanin and M. Nica, "Finite depth and width corrections to the neural tangent kernel," *arXiv preprint arXiv:1909.05989*, 2019.
- [34] J. Lee, L. Xiao, S. Schoenholz, Y. Bahri, R. Novak, J. Sohl-Dickstein, and J. Pennington, "Wide neural networks of any depth evolve as linear models under gradient descent," in *Advances in neural information processing systems*, 2019, pp. 8572–8583.
- [35] L. Xiao, J. Pennington, and S. S. Schoenholz, "Disentangling trainability and generalization in deep learning," *arXiv preprint arXiv:1912.13053*, 2019.
- [36] M. Raghu, B. Poole, J. Kleinberg, S. Ganguli, and J. Sohl-Dickstein, "On the expressive power of deep neural networks," in *international conference on machine learning*. PMLR, 2017, pp. 2847–2854.
- [37] T. Serra, C. Tjandraatmadja, and S. Ramalingam, "Bounding and counting linear regions of deep neural networks," in *International Conference on Machine Learning*. PMLR, 2018, pp. 4558–4566.

[38] B. Hanin and D. Rolnick, "Complexity of linear regions in deep networks," *arXiv preprint arXiv:1901.09021*, 2019.

[39] H. Xiong, L. Huang, M. Yu, L. Liu, F. Zhu, and L. Shao, "On the number of linear regions of convolutional neural networks," *arXiv preprint arXiv:2006.00978*, 2020.

[40] Y. Jiang, B. Neyshabur, H. Mobahi, D. Krishnan, and S. Bengio, "Fantastic generalization measures and where to find them," *arXiv preprint arXiv:1912.02178*, 2019.

[41] Y. Lee, J. Lee, S. J. Hwang, E. Yang, and S. Choi, "Neural complexity measures," 2020.

[42] T. Unterthiner, D. Keysers, S. Gelly, O. Bousquet, and I. Tolstikhin, "Predicting neural network accuracy from weights," *arXiv preprint arXiv:2002.11448*, 2020.

[43] G. Huang, Z. Liu, L. Van Der Maaten, and K. Q. Weinberger, "Densely connected convolutional networks," in *Proceedings of the IEEE conference on computer vision and pattern recognition*, 2017, pp. 4700–4708.

[44] R. Burkholz and A. Dubatovka, "Initialization of relus for dynamical isometry," in *Advances in Neural Information Processing Systems*, 2019, pp. 2385–2395.

[45] S. Hayou, A. Doucet, and J. Rousseau, "On the impact of the activation function on deep neural networks training," *arXiv preprint arXiv:1902.06853*, 2019.

[46] Y. Shin and G. E. Karniadakis, "Trainability of relu networks and data-dependent initialization," *Journal of Machine Learning for Modeling and Computing*, vol. 1, no. 1, 2020.

[47] C. Wang, G. Zhang, and R. Grosse, "Picking winning tickets before training by preserving gradient flow," *arXiv preprint arXiv:2002.07376*, 2020.

[48] H. Li, Z. Xu, G. Taylor, C. Studer, and T. Goldstein, "Visualizing the loss landscape of neural nets," *arXiv preprint arXiv:1712.09913*, 2017.

[49] A. Jacot, F. Gabriel, and C. Hongler, "Neural tangent kernel: Convergence and generalization in neural networks," in *Advances in Neural Information Processing Systems 31*, 2018.

[50] L. Chizat, E. Oyallon, and F. Bach, "On lazy training in differentiable programming," 2019.

[51] K. He, X. Zhang, S. Ren, and J. Sun, "Delving deep into rectifiers: Surpassing human-level performance on imagenet classification," in *Proceedings of the IEEE international conference on computer vision*, 2015, pp. 1026–1034.

[52] N. Cohen, O. Sharir, and A. Shashua, "On the expressive power of deep learning: A tensor analysis," in *Conference on learning theory*. PMLR, 2016, pp. 698–728.

[53] F. Croce, M. Andriushchenko, and M. Hein, "Provable robustness of relu networks via maximization of linear regions," in *the 22nd International Conference on Artificial Intelligence and Statistics*. PMLR, 2019, pp. 2057–2066.

[54] B. Hanin and D. Rolnick, "Deep relu networks have surprisingly few activation patterns," in *Advances in Neural Information Processing Systems*, 2019, pp. 361–370.

[55] R. Giryes, G. Sapiro, and A. M. Bronstein, "Deep neural networks with random gaussian weights: A universal classification strategy?" *IEEE Transactions on Signal Processing*, vol. 64, no. 13, pp. 3444–3457, 2016.

[56] A. Gaier and D. Ha, "Weight agnostic neural networks," *arXiv preprint arXiv:1906.04358*, 2019.

[57] V. Ramanujan, M. Wortsman, A. Kembhavi, A. Farhadi, and M. Rastegari, "What's hidden in a randomly weighted neural network?" in *Proceedings of the IEEE/CVF Conference on Computer Vision and Pattern Recognition*, 2020, pp. 11893–11902.

[58] K. Bhardwaj and R. Marculescu, "Towards unifying neural architecture space exploration and generalization," 2019.

[59] J. You, J. Leskovec, K. He, and S. Xie, "Graph structure of neural networks," *arXiv preprint arXiv:2007.06559*, 2020.

[60] S. Arora, S. S. Du, W. Hu, Z. Li, R. Salakhutdinov, and R. Wang, "On exact computation with an infinitely wide neural net," *arXiv preprint arXiv:1904.11955*, 2019.

[61] Y. Shu, W. Wang, and S. Cai, "Understanding architectures learnt by cell-based neural architecture search," in *International Conference on Learning Representations*, 2019.

[62] I. Radosavovic, J. Johnson, S. Xie, W.-Y. Lo, and P. Dollár, "On network design spaces for visual recognition," in *Proceedings of the IEEE/CVF International Conference on Computer Vision*, 2019, pp. 1882–1890.

[63] I. Radosavovic, R. P. Kosaraju, R. Girshick, K. He, and P. Dollár, "Designing network design spaces," in *Proceedings of the IEEE/CVF Conference on Computer Vision and Pattern Recognition*, 2020, pp. 10428–10436.

[64] R. J. Williams, "Simple statistical gradient-following algorithms for connectionist reinforcement learning," *Machine learning*, vol. 8, no. 3–4, pp. 229–256, 1992.

[65] Z. Yan, X. Dai, P. Zhang, Y. Tian, B. Wu, and M. Feiszli, "Fp-nas: Fast probabilistic neural architecture search," in *Proceedings of the IEEE/CVF Conference on Computer Vision and Pattern Recognition*, 2021, pp. 15139–15148.

[66] L. Li and A. Talwalkar, "Random search and reproducibility for neural architecture search," in *Uncertainty in Artificial Intelligence*. PMLR, 2020, pp. 367–377.

[67] P. Chrabaszcz, I. Loshchilov, and F. Hutter, "A downsampled variant of imagenet as an alternative to the cifar datasets," 2017.

[68] B. P. Carlin and T. A. Louis, "Empirical bayes: Past, present and future," *Journal of the American Statistical Association*, vol. 95, no. 452, pp. 1286–1289, 2000.

[69] B. Zoph, V. Vasudevan, J. Shlens, and Q. V. Le, "Learning transferable architectures for scalable image recognition," in *Proceedings of the IEEE conference on computer vision and pattern recognition*, 2018, pp. 8697–8710.

[70] S. Xie, H. Zheng, C. Liu, and L. Lin, "Snas: stochastic neural architecture search," *arXiv preprint arXiv:1812.09926*, 2018.

[71] H. Zhou, M. Yang, J. Wang, and W. Pan, "Bayesnas: A bayesian approach for neural architecture search," *arXiv preprint arXiv:1905.04919*, 2019.

[72] H. Cai, L. Zhu, and S. Han, "Proxylessnas: Direct neural architecture search on target task and hardware," *arXiv preprint arXiv:1812.00332*, 2018.

[73] X. Chen, L. Xie, J. Wu, and Q. Tian, "Progressive differentiable architecture search: Bridging the depth gap between search and evaluation," in *Proceedings of the IEEE International Conference on Computer Vision*, 2019, pp. 1294–1303.

[74] X. Chen and C.-J. Hsieh, "Stabilizing differentiable architecture search via perturbation-based regularization," *arXiv preprint arXiv:2002.05283*, 2020.

[75] D. Han, J. Kim, and J. Kim, "Deep pyramidal residual networks," in *Proceedings of the IEEE conference on computer vision and pattern recognition*, 2017, pp. 5927–5935.

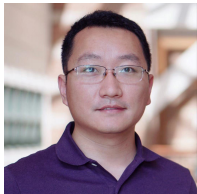
[76] M. Tan, B. Chen, R. Pang, V. Vasudevan, M. Sandler, A. Howard, and Q. V. Le, "Mnasnet: Platform-aware neural architecture search for mobile," in *Proceedings of the IEEE Conference on Computer Vision and Pattern Recognition*, 2019, pp. 2820–2828.



Wuyang Chen is a Ph.D. student in Electrical and Computer Engineering at University of Texas at Austin. He received his M.S. degree in Computer Science from Rice University in 2016, and his B.S. degree from University of Science and Technology of China in 2014. His research focuses on addressing domain adaptation/generalization, self-supervised learning, and AutoML.



Xinyu Gong is a Ph.D. student at the Department of Electrical and Computer Engineering, University of Texas at Austin. Before that, he obtained his Bachelor degree in Computer Science from the University of Electronic Science and Technology of China. He has also interned at Facebook AI, Horizon Robotics and Tencent AI Lab. His research interests are broadly in computer vision and machine learning, with a recent focus on neural architecture search.



Yunchao Wei is currently an Assistant Professor with the University of Technology Sydney. He received his Ph.D. degree from Beijing Jiaotong University, Beijing, China, in 2016. He was a Postdoctoral Researcher at Beckman Institute, UIUC, from 2017 to 2019. He is ARC Discovery Early Career Researcher Award Fellow from 2019 to 2021. His current research interests include computer vision and machine learning.



Humphrey Shi is an assistant professor in Department of Computer & Information Science, University of Oregon. Dr. Shi joins the UO from IBM's TJ Watson Research Center and the University of Illinois Grainger College of Engineering. His current research is at the intersection of computer vision and machine learning. Dr. Shi received awards from the Intelligence Advanced Research Projects Activity (IARPA) and winning multiple major international AI competitions such as the ImageNet video recognition challenge and the

Nvidia AI City Challenge.

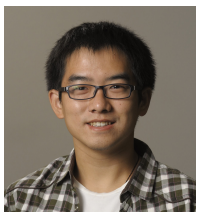


Zhicheng Yan Zhicheng Yan is a Staff Research Scientist at Facebook Research. He leads a team to develop a deep and personalized understanding of the objects and environment in the real world for improving Facebook AR products. Previously, he also worked on large-scale image and video understanding platforms. His research interests mainly include computer vision and machine learning. Zhicheng received his Ph.D from Department of Computer Science, University of Illinois at Urbana-Champaign in 2016. His

supervisor is Prof. Yizhou Yu. Before that, he was a master student in the College of Computer Science and Technology, Zhejiang University and a research assistant of State Key Lab of CAD&CG. His supervisor is Prof. Wei Chen. Zhicheng completed his Bachelor's degree at Zhejiang University majoring in Software Engineering in July, 2007.



Yi Yang is currently a Professor with the University of Technology Sydney. He received his Ph.D. degree from Zhejiang University, Hangzhou, China, in 2010. He was a post-doctoral researcher in the School of Computer Science, Carnegie Mellon University. His current research interests include machine learning and its applications to multimedia content analysis and computer vision, such as multimedia retrieval and video content understanding.



Zhangyang Wang is currently an Assistant Professor of ECE at UT Austin. He was an Assistant Professor of CSE, at TAMU, from 2017 to 2020. He received his Ph.D. in ECE from UIUC in 2016, and his B.E. in EEIS from USTC in 2012. Prof. Wang is broadly interested in the fields of machine learning, computer vision, optimization, and their interdisciplinary applications. His latest interests focus on automated machine learning (AutoML), learning-based optimization, machine learning robustness, and efficient deep learning.